# EiHi Net: Out-of-Distribution Generalization Paradigm

Qinglai Wei[1], Beiming Yuan[1], Diancheng Chen[*]

*School of Artificial Intelligence, University of Chinese Academy of Sciences, Beijing 100049, China*

*State Key Laboratory for Management and Control of Complex Systems, Institute of Automation, Chinese Academy of Sciences, Beijing 100190, China*

**Abstract**

This paper develops a new EiHi net to solve the out-of-distribution (OoD) generalization problem in deep learning. EiHi net is a model learning paradigm that can be blessed on any visual backbone. This paradigm can change the previous learning method of the deep model, namely find out correlations between inductive sample features and corresponding categories, which suffers from pseudo correlations between indecisive features and labels. We fuse SimCLR and VICReg via explicitly and dynamically establishing the original - positive - negative sample pair as a minimal learning element, the deep model iteratively establishes a relationship close to the causal one between features and labels, while suppressing pseudo correlations. To further validate the proposed model, and strengthen the established causal relationships, we develop a human-in-the-loop strategy, with few guidance samples, to prune the representation space directly. Finally, it is shown that the developed EiHi net makes significant improvements in the most difficult and typical OoD dataset Nico, compared with the current SOTA results, without any domain (*e.g.* background, irrelevant features) information.

*Keywords:* Deep learning, out-of-distribution, diversity shift, correlation shift, domain shift.

---

[*]Email Addresses: qinglai.wei@ia.ac.cn (Q. Wei), yuanbeiming20@mails.ucas.ac.cn (B. Yuan), chendiancheng2020@ia.ac.cn (D. Chen)

[*]Corresponding author

[1]Equal Contribution.

## 1. Introduction

It goes without saying that the excellent performance of traditional deep learning algorithms [1, 2] when the samples of training and test sets are independent and identically distributed (IID) [3, 4, 5, 6]. However, this assumption on the samples of training and test sets is fragile and easy to break, and when it disappears, deep models show a decline in performance in several tasks [7, 8]. Tracking down the culprit of decline leads to the fact that, traditional deep learning algorithms are based on the learning method of inducing correlation between features and categories. When the test data is out-of-distribution (OoD), the knowledge summarized by the deep learning algorithm on the training set is difficult to generalize [9, 10]. However, the OoD problem has little impact on humans, we believe that it is closely related to the way humans learn, which is different from deep learning models. When determining the category of objects, humans are capable of filtering irrelevant background information and looking for unique features. In view of this situation, we designed two paradigms to solve the problem of OoD, by mimicking human learning style, and starting from two key OoD factors, namely diversity shift and correlation shift [11]. Diversity shift refers to the offset between the domains of the training set and test set. Correlation shift refers to the offset of the domains in the training set. Non- I.I.D. Image dataset with Contexts (NICO) [12] carries these two Ood factors comprehensively. We will describe in detail how these two factors impede the performance of traditional deep learning algorithms in image classification tasks. We noticed that children learn to distinguish various animals through mediums like cartoon cards and photos under proper guidance. This process gives us the inspiration for designing the EiHi (**E**liminate **i**rrelevant features with **h**uman **i**ntervention) network. To be specific, we formulate two paradigms to solve the OoD problem, which can be blessed on any backbone to solve the classification task. We also designed some challenges. The original setting of the

2

NICO dataset is to train 8 domains and test 2 domains. This paper attempts to train 7 domains and test 3 domains to challenge the stronger diversity shift case. For the challenge of correlation shift, we enhanced the strength of domains shift to observe the performance of the EiHi net.

## 2. Problem Description

Deep learning suffers from out-of-distribution (OoD) problems for a long time. At present, there are two common OoD factors [11], the first is diversity shift. When a trained model faces a situation where the object appears in a completely new domain, the model usually shows poor performance. For instance, the trivial model is trained to identify the presence of sheep, but our training data never had sheep standing in the snow. Thus, the model would not perform well in identifying whether there are sheep in the snow background, we will give experiments in this section to show this situation. The NICO (He, Shen, and Cui 2020) data set has described this problem well [12].

Another common OoD factor reported in the NICO data set is correlation shift [13, 14]. This factor will also bring fatal damage to the performance of the deep learning algorithm, such that the biased distribution usually causes the pseudo correlation between the domain and the object information [11]. For example, most sheep data acquisition takes place on grasslands, and this situation will cause a pseudo correlation between grassland and the sheep's own features, as most of the samples with "sheep" labels contain grassland and sheep simultaneously. In traditional image classification tasks, the deep learning model trained by the cross-entropy loss function takes the correlation between sample features and classes as the basis of sample classification tasks [8, 15], and cannot encode features of the target in the desired way. On the sample group with a correlation shift problem, the model will inevitably pay attention to pseudo correlation. But as a feature of sheep image data, the grasslands should not be associated with the existence of sheep.

Next, we describe the diversity shift problem from the experimental perspec-

tive based on the NICO-animal and the NICO-vehicle data set. There are 10 types of animals in the NICO-animal dataset, and each animal has 10 domains, including the background and pose of the animal. There are 9 types of vehicles in the Nico-vehicle dataset, and each type of vehicle has 10 domains, including the scene and style. Some examples of the NICO-animal and NICO-vehicle are shown in Figures 1 and 2. 8 domains as randomly chosen as the source domains, and the remaining 2 domains as target domains. We first train and test the deep learning model on the mixed data of all domains, and take the test accuracies as the benchmark. We then train the model with the source domain data and test it on data from the target domains, and compare the test results with the benchmark to observe the impact of domain division as the first experiment. To ensure the fairness of the experiment, we keep the scale of training sets and test sets consistent in all experimental setups. The experimental results are shown in Table 1. For the test results, we are surprised by the performance of the Resnet series, which may be due to the failure to import pre-training parameters or the limited scale of Nico data.

Table 1: Experiment of Domain Shift Impact (8:2)

| dataset | model | Domain mixing(10:10) | Domain shift(8:2) |
|---|---|---|---|
| NICO-Animal | ResNet18 | 41.03±0.10% | 28.56±0.30% |
| | ResNet50 | 54.55±0.15% | 39.55±0.25% |
| | Vgg16 | 62.49±0.21% | 48.66±0.50% |
| | Vgg19 | 60.22±0.13% | 46.11±0.09% |
| NICO-Vehicle | ResNet18 | 53.45±0.12% | 42.29±0.08% |
| | ResNet50 | 70.20±1.18% | 55.16±0.35% |
| | Vgg16 | 74.13±1.33% | 58.24±0.40% |
| | Vgg19 | 74.59±1.26% | 57.60±0.80% |

In the experiment of investigating the influence of correlation shift [13, 14], we magnify this phenomenon by randomly reducing samples in some training sets. Specifically, we select one of the 8 source domains as the primary domain and reduce the number of samples in the other domains to 1/5 of the primary one as the secondary domain. The reduced 8 source domains are used for training,
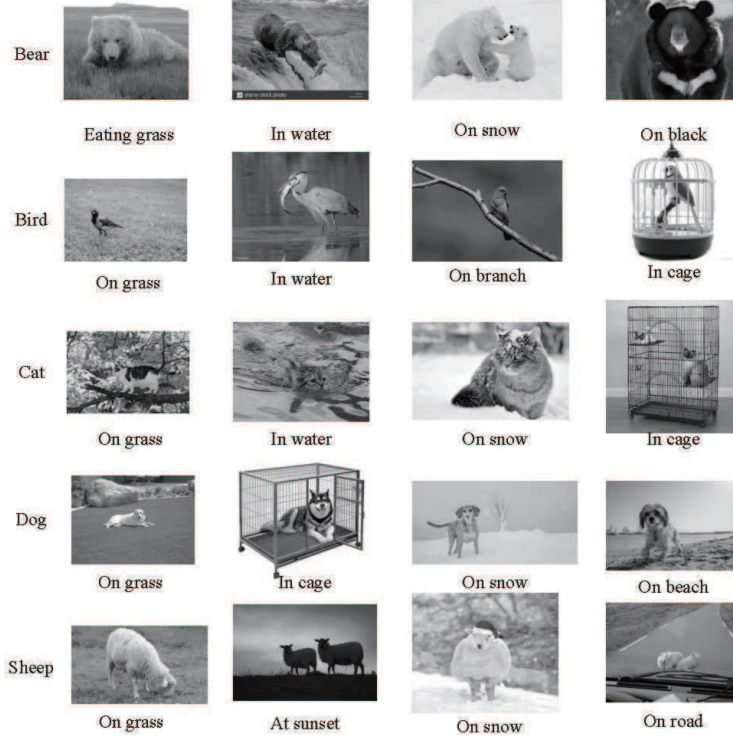
Figure 1: The figure shows the example of NICO-animal.

the target domain is left unchanged. The experimental results of vgg16 on NICO with stronger domain shift are shown in Table 2, and make it as the benchmark for the correlation shift problem.

Because prevalent pre-training(e.g. ImageNet pre-training model) will cover most of the information needed in our experiment, all of our experiments will not adopt the pre-training scheme. We conduct experiments 5 times, and the model with the highest accuracy in the training set is used for testing. We take the average of the 5 results as the test results.
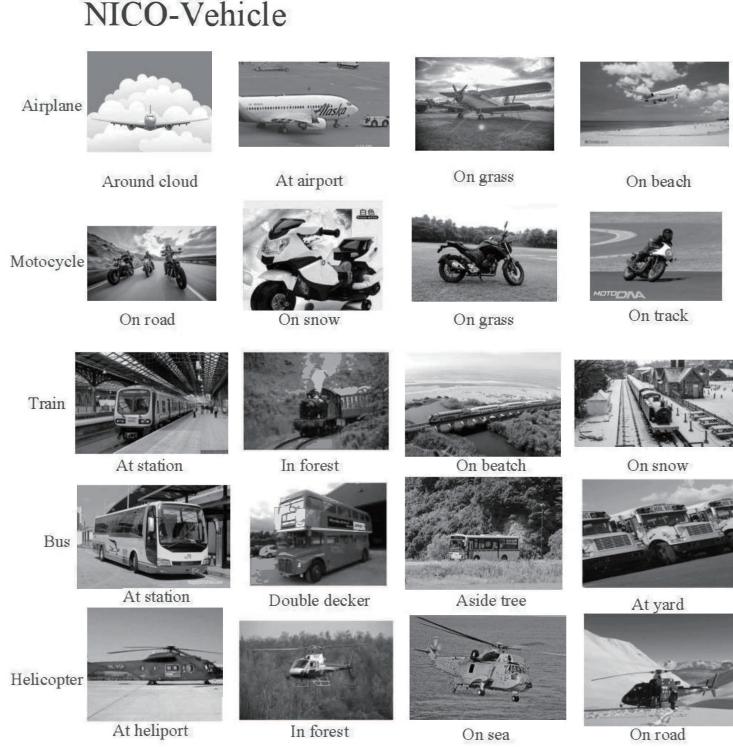
Figure 2: The figure shows the example of NICO-vehicle.

## 3. Related works

In this section, we will briefly introduce the research status of the OoD problem.

**NICO dataset [12]:** The problem of OoD image classification has not been studied to a great extent. A key reason is the lack of well-designed data sets to support relevant research. The NICO dataset visualizes the problem of OoD image classification. It uses context to consciously create Non-Independent and Identically Distributed (Non-IID) data. Compared with other data sets, NICO can support various Non-IID situations with sufficient flexibility. As mentioned earlier, two kinds of OoD factors, diversity shift and correlation shift, which are fatal to the traditional deep learning model, are well reflected in the NICO data set. A lot of work has contributed to eliminating the influence of these factors,

Table 2: Vgg16 on nico 8:2 with domain shift 5:1:1:1:1:1:1:1

| dataset | model | original (8:2) | Stronger domain shift (8:2) |
|---------|-------|----------------|-----------------------------|
| NICO-Animal | vgg16 | 48.66±0.50% | 37.83±0.12% |
| NICO-vehicle | vgg16 | 58.24±0.40% | 41.85±0.25% |

*e.g.* domain adaptation and covariate shift methods [16, 17, 18]. These works can obtain good performance, but they are not feasible in practice, because they need the test data distribution as a priori knowledge. The literature publishing NICO data sets also systematically expound on the impact of the OoD problem on the traditional deep learning model. We believe that NICO is an OoD dataset that takes into account both difficulty and typicality. In [12], the author compared multiple Non-I.I.D datasets horizontally, and finally found that only the NICO can support the different types of Non-IID. research with robust and explainable machine learning [19, 20, 21, 22]. Therefore, the excellent NICO data set has become our focus in this paper.

**Stable learning [23]:** Models that minimize the empirical error of training data do not necessarily perform well on test data, which leads to the challenge of Non-IID learning. When the training samples do not provide enough information to approximate the training distribution itself, the problem is more serious. StableNet, proposed by Cui Peng in 2021, provides a novel method to solve such problems. The shift domain distribution in the samples is forcibly corrected by weighting the sample. The correlation between sample features is reduced by sample weighting, and the amount of calculation required to control the correlation of sample features by HSIC-loss is avoided.

**Dec Aug [11]:** Traditional methods either assume the known heterogeneity of training data (such as domain labels) or assume that the capacities of different domains are roughly equal. DecAug analyzed two kinds of OoD factors contained in Nico data, describing Nico as a two-dimensional Ood problem and expounding the necessity of adding a domain label. By introducing domain labels, DecAug arranges the deep learning model to extend two branches to learn

domain information and object information in the sample, respectively. In addition, DecAug arranges the learning directions of the parameters of the two branches to be perpendicular, in order to ensure that the information learned by each of these two branches is as pure and decoupled as possible. However, we think this is inappropriate. The introduction of domain labels increases the workload of label data. In addition, many domains are difficult to label as clearly as objects. We can clearly label sheep as "sheep", but it is difficult to clearly label the background mixed with streams and grasslands. It is also difficult to unify and collect domain tags, which has become a problem in this method.

**SimCLR [24]:** SimCLR simplifies the recently proposed comparative self-supervised learning algorithm and does not need a special architecture (*e.g.* asymmetric twin structure) or memory bank. There are three points in SimCLR: the combination of data amplification plays a key role in defining effective prediction tasks; A learnable nonlinear transformation is introduced between representation and contrast loss, which greatly improves the quality of representation learning; Compared with supervised learning, comparative learning benefits from larger batches and more training steps. The loss function $info\_nce$ in SimCLR is also adopted in this paper. Two independent data amplification operators are extracted from the same augmentation methods and applied to each data example in a batch to obtain two related views. The basic encoder network $f(\cdot)$ and projection head $g(\cdot)$ are trained to maximize consistency by using the contrast loss. After the training, we eliminate the projection head $g(\cdot)$, and only use the encoder $f(\cdot)$ to complete the downstream task.

**Barlow Twins [25]:** Barlow Twins is a self-supervised learning method. For self-supervised learning, a very useful method is to learn the embedding vector, because it is not affected by the distortions of input samples. However, there is also an unavoidable problem: trivial constant solutions. The simple explanation of trivial constant solutions is that no matter what kind of input, the output of the neural network is a constant value. At present, most methods try to avoid this problem with a lot of clever methods. Barlow twins pro-

pose an objective function, which measures the cross-correlation matrix between the sample's and its distortion's feature representation (embedding vector). Ir makes the cross-correlation matrix as close to the identity matrix as possible, so as to avoid the occurrence of collapse. This makes the sample similar to its distorted embedding vectors, provides feature representation and minimizes the redundancy between these vectors. Barlow twins do not require large batches or asymmetry between network twins (such as practice network, gradient stopping, etc.), which benefits from very high-dimensional output vectors.

**VICReg [26]:** The self-monitoring method for image representation learning is generally based on the consistency between the embedding vectors of the same image and different views. The author introduces VICReg (Variance-Invariance-Covariance Regularization), which has a simple regularization term on the embedded variance of each dimension, so it can clearly avoid the occurrence of the collapse problem. VICReg combines the variance term with the decorrelation mechanism based on reducing redundancy and covariance regularization, and has achieved results equivalent to the current technical level in several downstream tasks. The distance between two feature representations from the same image is minimized, the variance of each feature representation in a batch remains above the threshold, and the covariance between each dimension of all feature representations in a batch approaches, which makes these feature representations more decoupled and prevents collapse. In a nutshell, VICReg learns different feature representations for all samples in the batch, and decouples each dimension of the representations. The ability of VICReg coding features is not affected by sample distortion.

## 4. Core feature extraction

We're amazed at how children learn. Using fewer data, such as cards with animal pictures, they can learn to identify animals in any scene. Imagine a scene where a child's parents hold an animal learning card, point to the cow on it, and describe "the one with horns is the cow". In this scenario, We believe that

9

there are two key points for children to learn effectively using limited data. The first key is to point out which features are unique to one class, and can be used to distinguish objects. The second key is the partition of features, removing those that do not belong to the object but can still be summarized as unique features in the sample group, *e.g.*, pseudo-relevant features [8, 15].

In image classification tasks, traditional CNNs (convolutional neural networks) are usually composed of stacked convolutional layers and stacked fully connected neural networks, such as the ResNet [2] series and Vgg [19] series. The stacked convolution layer usually plays the role of capturing the features of the image. In the following, we also call these layers feature capture networks. The features in the image will activate a part of the convolution kernels contained in the convolution layer to produce the feature representation of the image. The stacked full connection layer usually makes decisions based on the feature representation. We design two paradigms to work on the above-mentioned procession. This section introduces the first paradigm we use, pair-wise contrastive learning. We use it to guide the training of the feature capture network so that the network can summarize the desired features.

We hope to give hints to the feature capture network by training it through contrastive learning. These hints are included in the process of comparing the original sample with positive and negative samples. We hope that these hints will enable the network to find proper features belonging to each class. Since we believe that in the process of summarizing the same features between the samples belonging to identical categories (positive samples), the object information of the samples will be retained, and the domain information will be gradually abandoned. When summarizing differences between samples with negative samples, the object information retained through positive samples comparison will be further refined. This paper holds that finding the unique features among samples belonging to the same class can offset some of the correlation shift and diversity shift problems, because the unique features will not be contained in the domain information. We then summarize the correlation between unique features and sample categories, which will be less affected by domain informa-

10

tion.

The unsupervised learning method, VICReg [26], is an excellent comparative learning method, which sets up positive and negative samples explicitly and inexplicitly, respectively. However, this method is not suitable for solving the OoD problem. For the comparison of the positive samples, VICReg sets the invariance loss term. This term compares the features of the samples' different distortions. VICReg does not compare samples of the same class to achieve a fully unsupervised image feature encoding manner, which is different from our purpose. Meanwhile, VICReg sets the variance loss term, which serves as a positive-negative sample pair comparator. The implication of this term is that the learned representations of samples in a batch should be different, which is unfriendly to different samples belonging to the same class in a batch. Variance term treats positive samples as negative counterparts, which occurs frequently in the mini-size data set. Furthermore, VICReg prevents the network from outputting trivial constant solutions by setting covariance term constraint, so that the information of each dimension in sample feature representation is uncorrelated. The covariance loss term expects a larger batch size, but such a size will induce more positive samples to be treated as negative samples by the variance term, which is a contradictory. ADACLR (zhang, Yan and Yang 2020) [20] also mentioned these issues. We will solve that by explicitly setting positive and negative samples in a supervised way.

Instead of connecting the supervised downstream tasks to the unsupervised feature capture network, it is better to explicitly set positive and negative samples based on the object label to train the feature capture network. This process does not provide additional supervisory signals. We set different samples of the same class to be positive samples, and the samples from other classes naturally become negative counterparts. We believe that setting a positive sample in this way can make the network summarize commonalities better, rather than just improving the network's ability to resist distortion. In addition, The artificial setting of positive and negative samples also effectively solves the batch size contradiction induced by the covariance and variance term. No matter how

11

large the batch size is, there will be no situation where the positive sample is regarded as a negative one.

We choose $info\_nce$ to formulate the coding method of the feature capture network instead of the variance and invariance terms in VICReg. We have explained the batch size contradiction induced by variance loss terms before. In addition, when applying invariance loss item to our supervised positive sample setting method, requiring different samples to be encoded into identical features will induce the network to output the trivial constant solution, since such requirements are too tough for the network. For instance, the two distortions of a white cat picture can be easily encoded into an identical feature representation by a network, but it is difficult to encode the pictures of a white cat and a black cat with different poses. loss Thus, we propose to use $\ell_{\text{info\_nce}}(\cdot)$ in Equation (1) to replace variance and invariance terms, and keep covariance of VICReg unchanged. We use $\ell_{\text{info\_nce}}\left(Z_{ori}, Z_{pos}, Z_{neg^1}, Z_{neg^2}, ..., Z_{neg^M}\right)$ to make the vector directions of $Z_{ori}$ and $Z_{pos}$ to be identical, and the vector directions of $Z_{ori}$ and $Z_{neg^m}$ to be vertical. In this way, we normalize the encoded feature representation as the embedding vector of the sample. By constraining the vector direction of the encoded feature representations can we effectively prevent trivial constant solutions in the network. The network is abstracted as $f_\theta(\cdot)$, thus, $z = f_\theta(x)$, where $z \in R^d$ is the feature representation of input $x \in R^{c \times h \times w}$. Our loss function setting is shown in the following equation

$$
\ell\left(Z_{ori}, Z_{pos}, Z_{neg^1}, Z_{neg^2}, ..., Z_{neg^M}\right)
$$
$$
= \lambda \ell_{\text{info\_nce}}\left(Z_{ori}, Z_{pos}, Z_{neg^1}, Z_{neg^2}, ..., Z_{neg^M}\right)
$$
$$
+ \ell_{\text{cov}}\left(Z_{ori}\right) + \ell_{\text{cov}}\left(Z_{pos}\right) + \ell_{\text{cov}}\left(Z_{neg}\right), \tag{1}
$$

where $Z_{neg} = concat\left(\{Z_{neg^m}\}_{m=1}^M\right)$, $Z_{ori} = concat\left(\{z_{ori_i}\}_{i=1}^n\right)$, $Z_{pos} = concat\left(\{z_{pos_i}\}_{i=1}^n\right)$, $Z_{neg^m} = concat\left(\{z_{neg^m_i}\}_{i=1}^n\right)$, $z_{ori_i}, z_{pos_i}, z_{neg^m_i} \in R^d$, $m \in [1, M], i \in [1, n]$. $Z_{ori}, Z_{pos}, Z_{neg^m}$ represents the feature representation

of small batch input $X_{ori} = concat\left(\{x_{ori_i}\}_{i=1}^n\right),\quad X_{pos} = concat\left(\{x_{pos_i}\}_{i=1}^n\right),$ $X_{neg^m} = concat\left(\{x_{neg^m}{}_i\}_{i=1}^n\right)$ $(x_{ori_i}, x_{pos_i}, x_{neg^m}{}_i \in R^{c \times h \times w})$. $x_{ori_i}$ stands for the $i$th original sample; $x_{pos_i}$ represent the sample belonging to the same class as the $x_{ori_i}$; $x_{neg^m}{}_i$ represents the $m$th sample belonging to different classes of $x_{ori_i}$. The function $\quad \ell_{\text{info\_nce}}\left(Z_{ori}, Z_{pos}, Z_{neg^1}, Z_{neg^2}, ..., Z_{neg^M}\right)$ is expressed as

$$\ell_{\text{info\_nce}}\left(Z_{ori}, Z_{pos}, Z_{neg^1}, Z_{neg^2}, ..., Z_{neg^M}\right) = -\frac{1}{n}\sum_{i=1}^n \left(\log\left(dis_i\right)\right), \qquad (2)$$

where

$$dis_i = softmax\left(\frac{dis_{pos_i}}{temper}, \frac{dis_{neg^1}{}_i}{temper}, \frac{dis_{neg^2}{}_i}{temper}, ...\frac{dis_{neg^M}{}_i}{temper}\right). \qquad (3)$$

The parameters $dis_{pos_i}$ and $dis_{neg^m}{}_i$, $m \in [1, M]$ are computed by $dis_{pos_i} = ||Z_{ori_i} \cdot Z_{pos_i}||_2$ and $dis_{neg^m}{}_i = ||Z_{ori_i} \cdot Z_{neg^m}{}_i||_2$, respectively. The parameter $temper \in R$ in Equation (3) is the temperature coefficient.

Next, we consider the function $\ell_{\text{cov}}(Z)$ in (1), which is designed as

$$\ell_{\text{cov}}(Z) = \frac{1}{d}\sum\left(\left(\frac{1}{n-1}\sum_{i=1}^n \left(Z_i - \overline{Z}\right)\left(Z_i - \overline{Z}\right)^T\right)^2 \cdot (1 - eye)\right) \qquad (4)$$

where

$$\overline{Z} = \frac{1}{n}\sum_{i=1}^n Z_i. \qquad (5)$$

The parameters $eye \in R^{d \times d}$ in Equation (4) is the identity matrix and the $\ell_{\text{cov}}(Z)$ eliminates the correlation in $z \in R^d$ different dimensions. We use $Z \in R^{n \times d}$, which is composed of a batch of $z$ to calculate $\ell_{\text{cov}}(Z)$. Denote $Z_{ori} \in R^{n \times d}$ to represent the $n$ independent random sampling results of $z_{ori} \in R^d$, and calculate the correlation value row-wise to form the covariance matrix. Adopting a ancestral sampling approach $X_{pos}$ and $X_{neg^m}$ in accordance to $X_{ori}$. Thus, we can only calculate $\ell_{\text{cov}}(Z)$, $\ell_{\text{cov}}(Z_{pos})$ and $\ell_{\text{cov}}(Z_{neg})$ separately. We

hope that $\ell_{\text{cov}}(\cdot)$ term helps the feature capture network trained under semi supervised learning to learn more uncorrlated features to prevent the feature capture network from dimensional collapse. We prefer to use Figure 3 to describe the feedforward process of input data in more detail.



$$\ell_{\text{info\_nce}}\left(\overline{Z}_{ori}, \overline{Z}_{pos}, \overline{Z}_{neg}\right) + \ell_{\text{cov}}\left(\overline{Z}_{ori}\right) + \ell_{\text{cov}}\left(\overline{Z}_{pos}\right) + \ell_{\text{cov}}\left(\overline{Z}_{neg}\right)$$
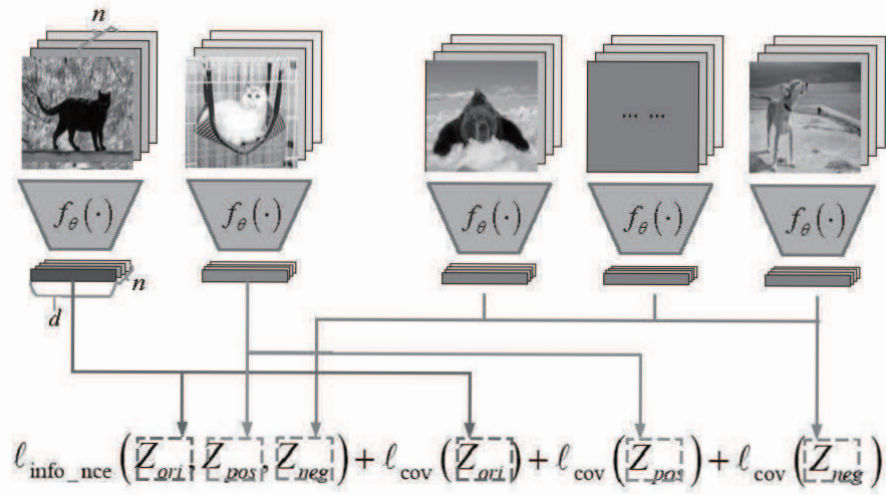
Figure 3: The figure shows the feedforward process of input data.

At the end of this section, we attach a simple comparative experiment to demonstrate the performance of using the first paradigm alone. The experimental data of this section directly adopts the data divided in the first experiment, that is, 8 source domains and 2 target domains. The pseudo-code for the comparative learning is shown in Algorithm 1. Our model is not initialized with any pre-trained model.

We train the feature capture network and fully connected non-linear discriminator separately, that is, the discriminator is trained with the fixed parameters of the feature capture network. In the experiment, one positive sample and five negative samples were selected to form a group with the original sample and we set the *temper* coefficient to 0.01. The model parameters with the highest accuracy during training are kept for the test. We run each test five times and keep the average results, as shown in Table 3. One should note that only category labels are available in our environment. This is different from DecAug and

14

---
**Algorithm 1:** the first stage of EiHi net

---
**Input:** Training set $D$, number of samples $n$,
        number of epoch $epoch$,
        proper backbone's **convolution layers**:$f_\theta\left(\cdot\right)$
**Output:** Trained $f_\theta\left(\cdot\right)$

1  **for** $i$ $in$ $(1,2,3,...,epoch)$ **do**
2     Take **samples** from $D$:
      $X_{ori} = [x_{ori_1}, x_{ori_2}, ...x_{ori_n}]$;
3     According to the category of each sample in $X_{ori}$, randomly select a
      **positive sample** in the same category :
      $X_{pos} = [x_{pos_1}, x_{pos_2}, ...x_{pos_n}]$;
4     According to the category of each sample in $X_{ori}$, $M$ **negative**
      **samples** are randomly selected from different categories:
      $X_{neg^m} = [x_{neg^m{}_1}, x_{neg^m{}_2}, ...x_{neg^m{}_n}]$;
5     **feed forward:**
      $Z_{ori} = f_\theta\left(X_{ori}\right)$;
      $Z_{pos} = f_\theta\left(X_{pos}\right)$;
6     **for** $m$ $in(1,2,...,M)$ **do**
7         **feed forward:**
          $Z_{neg^m} = f_\theta\left(X_{neg^m}\right)$;
8     **calculate:**
      $\ell = \ell\left(Z_{ori}, Z_{pos}, Z_{neg^1}, Z_{neg^2}, ..., Z_{neg^M}\right)$ by Equation (1)
      $\theta \leftarrow \theta - \alpha \cdot \frac{\nabla\ell}{\nabla\theta}$

---

its related work.

We hope to use the first paradigm to simulate the guidance of parents on the unique features when they teach their children to recognize animals.

## 5. Pseudo relevance elimination

As mentioned earlier in this paper, the fully connected layer (*e.g.* discriminator) of the traditional CNN (convolutional neural network) usually determines the category according to the features captured by the convolution layers. The traditional CNNs link features with labels with respect to the statistical relevance level. From the perspective of causality, this phenomenon makes the domain feature and label produce false causality [27, 28, 29], while the dataset with skewed domain distribution will lead to false relevance between domain features and labels, resulting in a wrong causal chain (the causal chain is shown in

Table 3: Core feature extraction experiment on NICO 8:2

| dataset | backbone | pure backbone(%) | only first paradigm(%) | training domains | test domians |
|---------|----------|------------------|------------------------|------------------|--------------|
| NICO-Animal | ResNet18 | 28.56±0.30 | **36.79±0.05** | 8 | 2 |
| | ResNet50 | **39.71±0.30** | 36.43±0.07 | 8 | 2 |
| | Vgg16 | 48.66±0.20 | **63.38±0.04** | 8 | 2 |
| | Vgg19 | 46.11±0.09 | **61.45±0.06** | 8 | 2 |
| NICO-Vehicle | ResNet18 | 42.29±0.08 | **49.89±0.09** | 8 | 2 |
| | ResNet50 | **55.16±0.35** | 47.82±0.05 | 8 | 2 |
| | Vgg16 | 58.24±0.40 | **68.09±0.14** | 8 | 2 |
| | Vgg19 | 57.60±0.80 | **70.42±0.06** | 8 | 2 |

Figure 4). Eliminating false causality and making domain information no longer participate in the induction process has become the primary task. Parents point to the location of the animal on the "animal card" to teach their children to identify the animal, which inadvertently completes the task. Therefore, we use the strategy of human-in-the-loop to provide some hints for the deep learning model to imitate the behavior that parents do.

We select very few samples (*e.g.*, 10 or 100, the volume is the same as the number of categories or multiplied by the number of categories and domains) to help eliminate the participation of domain features in the process of the sample category identification. We remove domain information from the selected samples $X_{sel}$, only retain object information, and bind the samples before and after deleting domain information as guidance samples $\{X_{sel}, X_{obj}\}$(where $X_{sel} = \{x_{sel_k}\}_{k=1}^{K}$, $X_{obj} = \{x_{obj_k}\}_{k=1}^{K}$, $x_{sel_k}, x_{obj_k} \in R^{c \times h \times w}$, $K$ is the number of selected samples).

In order to prevent the CNN from coupling the object features and domain features, we use Equation (4) to control the correlations between the features of samples. We extract the convolution layers of the CNN trained by the Equation (4) and cross-entropy loss as the feature capture network. Specifically, we input the guidance samples $\{X_{sel}, X_{obj}\}$ into the feature capture network to observe how the sample features change due to the elimination of background information. The dimensions of features whose values change significantly need to be

eliminated. We make criterion for dimensions which should be eliminated. The calculation process is shown as

$$Z_{guidance} = guidance\left(Z_{sel}, Z_{obj}, s\right) \tag{6}$$

where $Z_{sel}$ and $Z_{obj}$ represent the features of guidance sample $X_{sel} = \{x_{sel_k}\}_{k=1}^{K}$ and $X_{obj} = \{x_{obj_k}\}_{k=1}^{K}$, respectively. The parameter $s$ is a super parameter that specifies the maximum threshold for tolerable feature changes and $Z_{guidance} \in R^d$ is used to reflect which dimensions of the feature may summarize domain information. The function $guidance\left(Z_{sel}, Z_{obj}, s\right)$ is expressed as

$$guidance\left(Z_{sel}, Z_{obj}, s\right) = \sum_{k=1}^{K} chop\left(\frac{||z_{sel_k} - z_{obj_k}||}{||z_{sel_k}||}, s_k\right) \tag{7}$$

where $Z_{sel} = [z_{sel_1}, z_{sel_2}, ..., z_{sel_k}, ...z_{sel_K}]$, $Z_{obj} = [z_{obj_1}, z_{obj_2}, ..., z_{obj_k}, ...z_{obj_K}]$ $(z_{sel_k}, z_{obj_k} \in R^d)$. $s = [s_1, s_2, ..., s_k, ..., s_K]^T$, $s_k \in R$, and the function $chop\left(x, s\right)$ is expressed as

$$chop\left(x, s\right) = \left\{ \begin{array}{lll} 1: & if & x_i <= s \\ 0: & if & x_i > s \end{array} \right\} \tag{8}$$

where $x = [x_1, x_2, ..., x_i, ..., x_d]^T$, $x \in R^d$, $x_i \in R$, $s \in R$. The function $chop\left(x, s\right)$ will compare the value of each dimension (e.g. $x_i$) in the vector $x$ with the threshold $s$. If the value is higher than the threshold, it will be set to 0. Otherwise, it will be set to 1. $K$ paires of guidance samples $\{X_{sel}, X_{obj}\}$ use $chop\left(\cdot, s\right)$ to determine which dimensions of $Z_{guidance}$ are worth setting to 1. We adopt $Z_{guidance}$ to eliminate the encoded feature $Z_{features}$ to get $Z_{drop}$. Then, we let $Z_{drop}$ be calculated by

$$Z_{drop} = drop\left(Z_{features}, Z_{guidance}\right) \tag{9}$$

where $Z_{features} \in R^d$ is the feature encoded by the feature capture network,

and function $drop\left(Z_{features}, Z_{guidance}\right)$ is expressed as

$$drop\left(Z_{features}, Z_{guidance}\right) = Z_{features}[select(Z_{guidance} > 0)], \qquad (10)$$

where $Z_{drop} \in R^{\bar{d}}$, $\bar{d} <= d$. The $select(\cdot)$ operator in Equation (10) will check the value of each dimension in the vector and eliminate the dimensions that do not meet the conditions. We use this operator to eliminate the dimension with zero value of $Z_{guidance}$ in $Z_{features}$. $Z_{drop}$ is fed to a proper discriminator and trained for sample classification. We also use Algorithm 2 and Figure 5 to show this process in detail.
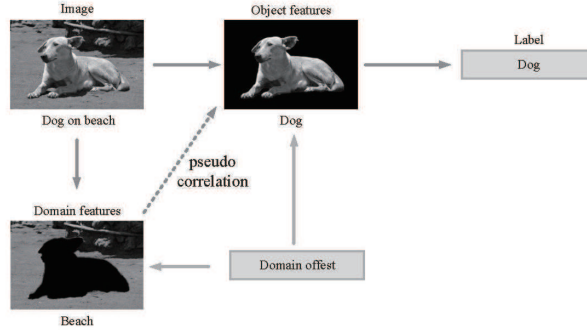


Figure 4: The domain offset factor leads to the generation of wrong causal chain.

We designed experiments to show the performance of the proposed paradigm in this section. We selected 10 samples in NICO-animal and 9 samples in NICO-vehicle as guidance samples, the amount of chosen samples are consistent with the number of categories. The dataset used is consistent with the previous experiment. The experimental results are shown in Table 4.

## 6. Methodology

We combine the core feature capture process and pseudo causal elimination process into our EiHi net. EiHi net can be blessed on any backbone to find the best match to solve the problem. And, we test Vgg and ResNet as backbones.

**Algorithm 2:** the second stage of EiHi net

---

**Input:** Training set $D$, number of samples $n$,
number of epoch $epoch$, drop scale $p$,
backbone trained by $\ell_{\text{cov}}$ and cross-entropy loss:$g_{\omega'}\left(f_\theta\left(\cdot\right)\right)$
**Output:** Trained backbone's **full connection layers:**$g_\omega\left(\cdot\right)$

**1** Take K **samples** from $D$:    $X = [x_1, x_2, ...x_K]$, where $K <<$ number of $D$

**2** Eliminate the domain information of sample $X$ to obtain one-to-one corresponding $X_{obj} = [x_{obj_1}, x_{obj_2}, ...x_{obj_K}]$

**3 feed forward:**
$Z = f_\theta\left(X\right)$;
$Z_{obj} = f_\theta\left(X_{obj}\right)$;

**4 calculate:**
$guid = \frac{||Z - Z_{obj}||}{||Z||}$    $guid \in R^{K \times d}$

**5 for** $k$ $in$ $(1, 2, 3, K)$ **do**

**6** $\quad$ $s_k = sort(guid_k)[\lfloor (1 - \text{p}) * \text{d} \rfloor]$

**7** $s = [s_1, s_2, ...s_k]$

**8 calculate:**
$Z_{guidance} = guidance\left(Z, Z_{obj}, s\right)$ by Equation (6)

**9 build:**
Construct fully connected neural network $g_\omega\left(\cdot\right)$,    where the input dimension of $g_\omega\left(\cdot\right)$ is the same as the number of vector $Z_{guidance}$ with values greater than 0, and the number of hidden layers is consistent with $g_{\omega'}\left(\cdot\right)$

**10 for** $i$ $in$ $(1, 2, 3, ..., epoch)$ **do**

**11** $\quad$ Take **samples and Labels** from $D$:
$\quad$ $X_{ori} = [x_{ori_1}, x_{ori_2}, ...x_{ori_n}]$;
$\quad$ $Y_{ori} = [y_{ori_1}, y_{ori_2}, ...y_{ori_n}]$;

**12** $\quad$ **feed forward:**
$\quad$ $Z_{ori} = f_\theta\left(X_{ori}\right)$;

**13** $\quad$ **for** $j$ $in$ $(1, 2, 3, ..., n)$ **do**

**14** $\quad\quad$ $z_{drop_j} = dorp\left(z_{ori_j}, Z_{guidance}\right)$ by Equation(9)

**15** $\quad$ $Z_{drop} = [z_{drop_1}, z_{drop_2}, ...z_{drop_n}]$;

**16** $\quad$ **feed forward:**
$\quad$ $out = g_\omega\left(Z_{drop}\right)$

**17** $\quad$ **calculate:**
$\quad$ $\ell = cross - entropy - loss\left(softmax\left(out\right), Y_{ori}\right)$
$\quad$ $\omega \leftarrow \omega - \alpha \cdot \frac{\nabla \ell}{\nabla \omega}$
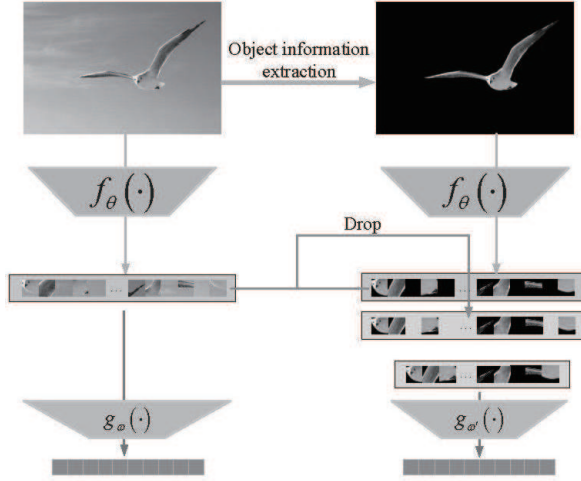
Figure 5: The figure shows the process of eliminating the domain information dimension.

Table 4: Context feature droping experiment on NICO 8:2

| dataset | backbone | pure backbone(%) | only second paradigm(%) | training domains | test domains |
|---|---|---|---|---|---|
| NICO-Animal | ResNet18 | 28.56±0.30 | **30.52±0.04** | 8 | 2 |
| | ResNet50 | 39.71±0.30 | **40.50±0.29** | 8 | 2 |
| | Vgg16 | 48.66±0.20 | **57.53±0.44** | 8 | 2 |
| | Vgg19 | 46.11±0.09 | **52.90±0.20** | 8 | 2 |
| NICO-Vehicle | ResNet18 | 42.29±0.08 | **49.27±0.27** | 8 | 2 |
| | ResNet50 | **55.16±0.35** | 52.05±0.30 | 8 | 2 |
| | Vgg16 | 58.24±0.40 | **63.52±0.14** | 8 | 2 |
| | Vgg19 | 57.60±0.80 | **64.44±0.06** | 8 | 2 |

The convolution layers and full connection layers of the backbone are trained by the two paradigms contained in the EiHi network respectively. The detailed algorithm process is shown in Algorithm 3. We list the test results of EiHi blessing on four backbones without pre-training on Nico dataset in table 5. We have also made a comparison of various algorithms. For comparison, we directly cite the average results of the StableNet on two NICO datasets recorded in [23]. The results of the comparison are shown in Table 6. In our experiment, only object labels are available.

We selected some samples in the training set and test set, and used EiHi

---
**Algorithm 3:** EiHi net
---

**Input:** Training set $D$, number of samples $n$,
number of epoch $epoch$, drop scale $p$,
proper backbone's **convolution layers**:$f_\theta(\cdot)$ ,
proper backbone's **full connection layers**:$g_\omega(\cdot)$,
number of guidance samples $K$

**Output:** Trained EiHi net $g_{\omega'}(f_\theta(\cdot))$

1  Take K **samples** from $D$:    $X = [x_1, x_2, ...x_K]$,
   where $K << $ number of $D$

2  Eliminate the domain information of sample $X$ to obtain one-to-one
   corresponding $X_{obj} = [x_{obj_1}, x_{obj_2}, ...x_{obj_K}]$

3  **training $f_\theta(\cdot)$ with Algorithm 1**
   $f_\theta(\cdot) = $ **Algorithm 1**$(D, n, epoch, f_\theta(\cdot))$

4  **feed forward:**
   $Z = f_\theta(X)$;
   $Z_{obj} = f_\theta(X_{obj})$;

5  **calculate:**
   $guid = \frac{||Z - Z_{obj}||}{||Z||}$    $guid \in R^{K \times d}$

6  **for** $k$ $in$ $(1, 2, 3, K)$ **do**

7  $\quad\lfloor$ $s_k = sort(guid_k)[\lfloor (1 - \mathrm{p}) * \mathrm{d} \rfloor]$

8  $s = [s_1, s_2, ...s_k]$

9  **calculate:**
   $Z_{guidance} = guidance(Z, Z_{obj}, s)$ by Formula (6)

10 **Pruning:**
   Eliminate the neurons in the input layer of $g_\omega(\cdot)$ until the number is
   the same as the number of vector $Z_{guidance}$ with values greater than 0,
   so as to obtain $g_{\omega'}(\cdot)$

11 **for** $i$ $in$ $(1, 2, 3, ..., epoch)$ **do**

12 $\quad$ Take **samples and Labels** from $D$:
   $\quad X_{ori} = [x_{ori_1}, x_{ori_2}, ...x_{ori_n}]$;
   $\quad Y_{ori} = [y_{ori_1}, y_{ori_2}, ...y_{ori_n}]$;

13 $\quad$ **feed forward:**
   $\quad Z_{ori} = f_\theta(X_{ori})$;

14 $\quad$ **for** $j$ $in$ $(1, 2, 3, ..., n)$ **do**

15 $\quad\quad\lfloor$ $z_{drop_j} = dorp(z_{ori_j}, Z_{guidance})$ by Equation(9)

16 $\quad$ $Z_{drop} = [z_{drop_1}, z_{drop_2}, ...z_{drop_n}]$;

17 $\quad$ **feed forward:**
   $\quad out = g_{\omega'}(Z_{drop})$

18 $\quad$ **calculate:**
   $\quad \ell = cross - entropy - loss(softmax(out), Y_{ori})$
   $\quad \omega' \leftarrow \omega' - \alpha \cdot \frac{\nabla \ell}{\nabla \omega'}$

Table 5: EiHi net on NICO 8:2

| dataset | backbone | pure backbone(%) | EiHi net(%) | training domains | test domians |
|---------|----------|------------------|-------------|------------------|--------------|
| NICO-Animal | ResNet18 | 28.56±0.30 | 37.42±0.06 | 8 | 2 |
| | ResNet50 | 39.71±0.30 | 37.21±0.09 | 8 | 2 |
| | Vgg16 | 48.66±0.20 | **64.41±0.05** | 8 | 2 |
| | Vgg19 | 46.11±0.09 | 62.80±0.04 | 8 | 2 |
| NICO-Vehicle | ResNet18 | 42.29±0.08 | 51.89±0.04 | 8 | 2 |
| | ResNet50 | 55.16±0.35 | 48.87±0.10 | 8 | 2 |
| | Vgg16 | 58.24±0.40 | 69.71±0.05 | 8 | 2 |
| | Vgg19 | 57.60±0.80 | **71.34±0.04** | 8 | 2 |

Table 6: various net on NICO 8:2

| data set | model | average accuracy | domain division |
|----------|-------|------------------|-----------------|
| NICO-Animal and NICO-Vehicle | JiGen | 54.72 | 8:2 |
| | M-ADA | 40.78 | 8:2 |
| | DG-MMLD | 47.18 | 8:2 |
| | RSC | 57.59 | 8:2 |
| | ResNet-18(pre-training) | 51.71 | 8:2 |
| | StableNet | <u>59.76</u> | 8:2 |
| | EiHi(ours) | **67.88** | 8:2 |

net to identify them. With the help of this identification process, we drew the saliency map [30] of EiHi net for each sample. Some examples of saliency maps are shown in Figures 6 and 7. Since the domain information in the test set has never appeared in the training set before, the saliency map result of the test set is better than that of the training set.

## 7. Challenge

The first challenge we tried was the greater diversity shift. We try to train 7 domains and test 3 domains in NICO to achieve an experimental setting with enhanced diversity shift. We observed and recorded the experimental results of the EiHi net blessing on four backbones. The experimental results are recorded in Table 7.

This paper tries to strengthen the correlation shift to create another challenge. We select **one** of the 8 source domains as the primary domain and set

Figure 6: The figure shows the saliency map of EiHi net for each NICO-Animal sample.

the other domains as the secondary domain for each class. We set the ratio of the number of primary domain samples to the number of secondary domain samples to 5:1. This ratio is based on the Adversarial setting in [23]. The original intention of the Adversarial setting is the same as the purpose of enhancing the correlation shift. Unfortunately, this setting is not attached to NICO in [23]. Based on this experimental setup, we observed and recorded the result five times, and recorded the average of the results in Table 8. Other model results appearing in Table 8 are from reference [12]. As the experimental difficulty increases, the number of negative examples is set to 8 and the temperature coefficient $temper$ is set to 0.01.

Figure 7: The figure shows the saliency map of EiHi net for each NICO-Vehicle sample.

We hope that more work on Nico in the future can also try to challenge these strengthened OoD problems.

## 8. Conclusion

In this paper, we propose the EiHi net, a paradigm that can be blessed on any backbone, to deal with the OoD generalization tasks. When using our paradigm to train the backbone, there is no need for additional domain labels and pre-training parameter loading. When only category labels are available, we achieve SOTA on the most difficult and representative two-dimensional OoD dataset NICO. Avoiding labeling domain information and inputting it into the

Table 7: EiHi net on NICO 7:3

| data set | model | pure backbone(%) | EiHi net(%) | Domain division |
|---|---|---|---|---|
| NICO-Animal | EiHi net (Vgg16) | 46.13±0.85 | **62.26±0.05** | 7:3 |
| NICO-Vehicle | EiHi net (Vgg16) | 55.62±1.60 | **62.72±0.08** | 7:3 |

Table 8: EiHi on NICO 8:2 with domain shift 5:1:1:1:1:1:1:1

| dataset | model | accuracy | Domain shift scale | Domain division |
|---|---|---|---|---|
| NICO-Animal | CNN | 37.17 | 5:1 | 8:2 |
| | CNN+BN | 38.70 | 5:1 | 8:2 |
| | CNBB | <u>39.06</u> | 5:1 | 8:2 |
| | pure backbone (vgg16) | 37.83 | 5:1 | 8:2 |
| | EiHi net (vgg16) | **57.68±0.05** | 5:1 | 8:2 |
| NICO-Vehicle | CNN | 40.61 | 5:1 | 8:2 |
| | CNN+BN | <u>41.98</u> | 5:1 | 8:2 |
| | CNBB | 41.41 | 5:1 | 8:2 |
| | pure backbone (vgg16) | 41.85 | 5:1 | 8:2 |
| | EiHi net (vgg16) | **57.86±0.09** | 5:1 | 8:2 |

deep learning model as a supervision signal not only saves manpower, but also allows for progress towards anthropomorphic intelligence. Our EiHi net can make the backbone extract the feature of samples more like human beings, so as to resist the OoD phenomenon presented by the sample set.

Adding more supervision signals can certainly make the deep model summarize more detailed correlations between features and labels. More detailed correlations induction will indeed reduce the impact of diversity shift and correlation shift. As DecAug does, it explicitly learns the object information and domain information of the sample by introducing category and domain labels simultaneously. We also believe that when the label is added to the pixel level,

the deep model will have amazing performance on OoD problems. However such skills that could improve performance to some extent do not reveal the essential law of intelligence. Therefore, we are concerned that this method of imitating people to extract image features is a more meaningful direction to solving the OoD generalization problem. "Intuitively, such mechanisms should be consistent with human cognitive habits, such as causality, possibly lighting up the way to the 'strong AI'[29]" which is also mentioned in [12], and EiHi net is an attempt in this direction. [31] mentioned that the method based on causal inference has an impressive effect on solving the long-tailed distribution of data sets, which also proves the effectiveness of the direction expected to be used on NICO. We believe that the original intention of NICO is not simply to make AI achieve higher scores to improve the influence of this discipline. In this paper, all experiments on the EiHi net do not set up a verification set, so our hyperparameters may not be in the best state, but we believe that solving problems from a meaningful direction can achieve better results without carefully adjusting them.

For future works, we will look for practical problems that have been plagued by the OoD generalization problem for a long time in the industry, so as to further improve the algorithm and apply it to practice.

## Reference

## References

[1] A. Krizhevsky, I. Sutskever, G. E. Hinton, Imagenet classification with deep convolutional neural networks, Advances in neural information processing systems 25 (2012) 1097–1105.

[2] K. He, X. Zhang, S. Ren, J. Sun, Deep residual learning for image recognition, in: Proceedings of the IEEE conference on computer vision and pattern recognition, 2016, pp. 770–778.

[3] S. Ren, K. He, R. Girshick, J. Sun, Faster r-cnn: Towards real-time object detection with region proposal networks, Advances in neural information processing systems 28 (2015) 91–99.

[4] Y. Ma, Y. He, F. Ding, S. Hu, J. Li, X. Liu, Progressive generative hashing for image retrieval., in: International Joint Conferences on Artificial Intelligence Organization, 2018, pp. 871–877.

[5] J. Li, X. Liu, M. Zhang, D. Wang, Spatio-temporal deformable 3d convnets with attention for action recognition, Pattern Recognition 98 (2020) 107037.

[6] A. Liu, X. Liu, J. Fan, Y. Ma, A. Zhang, H. Xie, D. Tao, Perceptual-sensitive gan for generating adversarial patches, in: Proceedings of the AAAI conference on artificial intelligence, Vol. 33, 2019, pp. 1028–1035.

[7] M. Arjovsky, L. Bottou, I. Gulrajani, D. Lopez-Paz, Invariant risk minimization, arXiv preprint arXiv:1907.02893 (2019).

[8] Z. Shen, P. Cui, T. Zhang, K. Kunag, Stable learning via sample reweighting, in: Proceedings of the AAAI Conference on Artificial Intelligence, Vol. 34, 2020, pp. 5692–5699.

[9] Y. Sun, X. Wang, Z. Liu, J. Miller, A. A. Efros, M. Hardt, Test-time training for out-of-distribution generalization (2019).

[10] D. Krueger, E. Caballero, J.-H. Jacobsen, A. Zhang, J. Binas, D. Zhang, R. Le Priol, A. Courville, Out-of-distribution generalization via risk extrapolation (rex), in: International Conference on Machine Learning, PMLR, 2021, pp. 5815–5826.

[11] H. Bai, R. Sun, L. Hong, F. Zhou, N. Ye, H.-J. Ye, S.-H. G. Chan, Z. Li, Decaug: Out-of-distribution generalization via decomposed feature representation and semantic augmentation, arXiv preprint arXiv:2012.09382 (2020).

[12] Y. He, Z. Shen, P. Cui, Towards non-iid image classification: A dataset and baselines, Pattern Recognition 110 (2021) 107383.

[13] S.-B. Chen, C. Ding, B. Luo, Y. Xie, Uncorrelated lasso, in: Twenty-seventh AAAI conference on artificial intelligence, 2013.

[14] M. Takada, T. Suzuki, H. Fujisawa, Independently interpretable lasso: A new regularizer for sparse regression with uncorrelated variables, in: International Conference on Artificial Intelligence and Statistics, PMLR, 2018, pp. 454–463.

[15] K. Kuang, R. Xiong, P. Cui, S. Athey, B. Li, Stable prediction with model misspecification and agnostic distribution shift, in: Proceedings of the AAAI Conference on Artificial Intelligence, Vol. 34, 2020, pp. 4485–4492.

[16] M. Long, H. Zhu, J. Wang, M. I. Jordan, Deep transfer learning with joint adaptation networks, in: International conference on machine learning, PMLR, 2017, pp. 2208–2217.

[17] E. Sangineto, G. Zen, E. Ricci, N. Sebe, We are not all equal: Personalizing models for facial expression analysis with transductive parameter transfer, in: Proceedings of the 22nd ACM international conference on Multimedia, 2014, pp. 357–366.

[18] C. Deng, X. Liu, C. Li, D. Tao, Active multi-kernel domain adaptation for hyperspectral image classification, Pattern Recognition 77 (2018) 306–315.

[19] Y. Shi, Y. Han, Q. Zhang, X. Kuang, Adaptive iterative attack towards explainable adversarial robustness, Pattern Recognition 105 (2020) 107309.

[20] D. Liu, L. Zhang, T. Luo, L. Tao, Y. Wu, Towards interpretable and robust hand detection via pixel-wise prediction, Pattern Recognition 105 (2020) 107202.

[21] M. Wu, M. Hughes, S. Parbhoo, M. Zazzi, V. Roth, F. Doshi-Velez, Beyond sparsity: Tree regularization of deep models for interpretability, in: Proceedings of the AAAI conference on artificial intelligence, Vol. 32, 2018.

[22] S. Muñoz-Romero, A. Gorostiaga, C. Soguero-Ruiz, I. Mora-Jiménez, J. L. Rojo-Álvarez, Informative variable identifier: Expanding interpretability in feature selection, Pattern Recognition 98 (2020) 107077.

[23] X. Zhang, P. Cui, R. Xu, L. Zhou, Y. He, Z. Shen, Deep stable learning for out-of-distribution generalization, in: Proceedings of the IEEE/CVF Conference on Computer Vision and Pattern Recognition, 2021, pp. 5372–5382.

[24] T. Chen, S. Kornblith, M. Norouzi, G. Hinton, A simple framework for contrastive learning of visual representations, in: International conference on machine learning, PMLR, 2020, pp. 1597–1607.

[25] J. Zbontar, L. Jing, I. Misra, Y. LeCun, S. Deny, Barlow twins: Self-supervised learning via redundancy reduction, in: International Conference on Machine Learning, PMLR, 2021, pp. 12310–12320.

[26] A. Bardes, J. Ponce, Y. LeCun, Vicreg: Variance-invariance-covariance regularization for self-supervised learning, arXiv preprint arXiv:2105.04906 (2021).

[27] J. Pearl, Causal inference in statistics: An overview, Statistics surveys 3 (2009) 96–146.

[28] Y. He, Z. Wang, P. Cui, H. Zou, Y. Zhang, Q. Cui, Y. Jiang, Causpref: Causal preference learning for out-of-distribution recommendation, in: Proceedings of the ACM Web Conference 2022, 2022, pp. 410–421.

[29] L. R. Goldberg, The book of why: The new science of cause and effect: by judea pearl and dana mackenzie, basic books (2018). isbn: 978-0465097609. (2019).

[30] K. Simonyan, A. Vedaldi, A. Zisserman, Deep inside convolutional networks: Visualising image classification models and saliency maps, arXiv preprint arXiv:1312.6034 (2013).

[31] B. Zhu, Y. Niu, X.-S. Hua, H. Zhang, Cross-domain empirical risk minimization for unbiased long-tailed classification, arXiv preprint arXiv:2112.14380 (2021).